

Theoretical Analysis of PM_{2.5} Mass Measurements by Nephelometry - #110

John V. Molenaar

Air Resource Specialists, Inc., 1901 Sharp Point Drive, Suite E, Fort Collins, CO 80525

ABSTRACT

With the recently promulgated PM_{2.5} mass standards, a need has appeared for continuous PM_{2.5} mass measuring instrumentation to complement standard filter based aerosol samplers. It is generally accepted that in most cases, the PM_{2.5} mass distribution and light scattering is dominated by particles with diameters in the size range 0.1–1.0 μ m. Early field studies indicated a reasonable correlation between gravimetric aerosol mass and integrating nephelometer measurements of aerosol scattering coefficient. Nephelometry is a mature science dating back 50 years with well understood design philosophies and inherent limitations. Nephelometers have proven to be capable of making highly accurate, precise continuous measurements of the aerosol scattering coefficient. In addition, nephelometers are very portable, rugged, requiring low maintenance and of moderate cost when compared to filter based aerosol samplers. These factors have lead to the reconsideration of employing size-cut nephelometers or light scattering photometers as surrogate continuous PM_{2.5} monitors. The main uncertainty is due to the fact that the measured aerosol scattering coefficient is not linearly proportional to aerosol mass, but rather a complex function of the ambient aerosol chemistry, shape, density, size distribution, and index of refraction as well as the optical properties and geometry of the nephelometer used. This paper uses Lorenz-Mie theory, reasonable estimates of the variation of ambient aerosol properties, and the optical characteristics of currently available nephelometers and light scattering photometers to investigate the theoretical limits of the accuracy and precision of PM_{2.5} mass measurements estimated by nephelometry.

INTRODUCTION

Before 1968, the general consensus was that since the physical characteristics of the ambient aerosol were so variable and unknown, no robust relationship between ambient aerosol concentration and measurable optical properties existed.¹ This view changed in 1968 when Charlson *et al.*² reported that to the contrary, a reasonable correlation was seen between gravimetric aerosol mass and the scattering coefficient measured with a newly developed closed chamber integrating nephelometer.³ This pioneering work initiated many measurement studies investigating the relationship between PM_{2.5} (diameter < 2.5 μ m) aerosol mass (M_f) and particle light scattering (b_{sp}).⁴⁻⁸ Additional studies made it clear that the PM_{2.5} ambient aerosol can be described by a lognormal volume distribution, with the aerosol mass and scattering coefficient dominated by particles in the accumulation mode, diameters in the size range 0.1–1.0 μ m.⁹⁻¹¹ The link between these two bulk physical parameters is the dry PM_{2.5} mass scattering efficiency: $\alpha_M = b_{sp,2.5}/M_f$. White has summarized these early field studies, reporting a range in α_M of 1.5-5.0m²/g.^{12,13} Early sensitivity analyses using Mie calculations indicated that α_M was expected to be weakly dependent on mass mean diameter and geometric standard deviation; and more strongly dependent on the index of refraction, and aerosol density.^{14,15,16} The wide variability in

reported α_M , from the early measurement and sensitivity studies, quickly lead to dropping the idea of using nephelometry as a $PM_{2.5}$ mass monitor. Instead, efforts focused on using Mie theory, measured scattering, measured aerosol size distributions, and rapidly improving chemical analyses in attempts to apportion scattering to individual chemical species.¹⁷⁻²⁵

The United States Environmental Protection Agency (U.S. EPA) has recently promulgated new $PM_{2.5}$ particle ambient concentration standards. The reference method for monitoring compliance with these standards is based on 24-hour gravimetric filter measurements of $PM_{2.5}$ mass.²⁶ Filter based measurements have a number of limitations:

1. The operating costs associated with making daily measurements will be high.^{26,27}
2. Inability of limited 24-hour integrated filter samples to evaluate spatial/temporal variations in human exposure to ambient air quality.^{28,29}
3. No real time information is available to local air quality agencies to issue alerts or implement control strategies.³⁰

In response to the above and other concerns, the use of nephelometry and light scattering photometry as a real-time continuous $PM_{2.5}$ aerosol monitoring instrument has re-emerged.^{27,31-33} The 1998 U.S.EPA report²⁷ combines the previously discussed studies and the more recent field experiments of particle scattering efficiencies empirically determined by collocating nephelometers with filter based samplers and states: “Data from a wide variety of urban, non-urban, and pristine environments imply that each $100Mm^{-1}$ of light scattering could potentially be associated with 8 to $34\mu g/m^3$ $PM_{2.5}$ in the atmosphere for 3 to 12-hour sampling durations.” This statement implies a range $2.9-12.5m^2/g$ for α_M . High α_M 's greater than 6.0 are due to the incorporation of high relative humidity scattering measurements into the analysis. Understanding this wide variation (a factor of 4) requires a reevaluation and extension of earlier sensitivity analyses of using nephelometry as a surrogate $PM_{2.5}$ mass monitor.

THEREORETICAL CALCULATIONS OF BULK SCATTERING/MASS RATIO (α_M)

Using Mie theory the light scattering per unit mass for a lognormal aerosol polydispersion can be calculated as:³⁴

Equation 1.

$$\alpha_M = (1.5 / \rho) \int_d Q_{scat}(n, k, d, \lambda) f(d, d_g, \sigma_g) / d \delta d$$

where:

$Q_{scat}(n,k,d,\lambda)$ is the Mie scattering efficiency at the wavelength of the scattered radiation (λ) for a single particle with complex refractive index $n-ik$, and diameter d .

The aerosol polydispersion $f(d,d_g,\sigma_g)$ is lognormal with a mass (volume) mean diameter d_g , geometric standard deviation σ_g , and average aerosol density ρ . The above equation demonstrates the main limitation of using light scattering measurements to determine aerosol

mass: one cannot distinguish whether a change in PM_{2.5} mass concentration (M_f), aerosol size distribution (d_g, σ_g), or aerosol physical properties (ρ, n, k), is causing the measured change in the detected scattered signal.

The natural variability of PM_{2.5} aerosol physical properties (ρ, n, k) has been studied by many investigators.³⁵⁻⁴² A review of this literature results in the following realistic ranges of physical properties (ρ, n, k) for the PM_{2.5} aerosol: $\rho = 1.0$ to 2.0g/cm^3 , $n = 1.3$ to 1.8 , and $k = 0.000$ to 0.200 . While the PM_{2.5} aerosol is now considered to be actually made up of at least two lognormal distributions,⁴³ for this sensitivity analysis it will assumed that the polydisperse PM_{2.5} aerosol can be adequately modeled as a single lognormal distribution with the following ranges of d_g and σ_g : $d_g = 0.05$ to $1.0 \mu\text{m}$ and $\sigma_g = 1.1$ to 3.0 .⁹⁻¹¹

To evaluate the theoretical effect of this variability on α_M , the scattering efficiency, Q_{scat} , at 550nm was computed using subroutines developed by Dave for all possible combinations of the parameters in the above ranges.⁴⁴ Table 1 lists the ranges and increments used for each physical and optical property. To avoid “pseudo-features” appearing in the Mie calculations, care was taken to use sufficiently small integration increments in all parameter bins to satisfy the Dave criterion.⁴⁵ It should be noted, this method of independent variation ignores the effect of correlations between parameters that may minimize the range of α_M for real particles, such as mineral particles (high density, transparent) in comparison to carbon particles (low density, absorbing). However, allowing the parameters to vary independently is a reasonable first step in the sensitivity analysis. It is also worth pointing out that, while in principle, Mie theory of scattering from polydispersions is applicable to only spherical particles, studies have indicated that it is a useful approximation to experimental measurements of PM_{2.5} particle scattering provided the size distribution is relatively broad.⁴⁶⁻⁴⁸

Table 1. Range, increment and number of steps in aerosol physical and optical properties used in Mie calculations.

Property	Range	Increment	Number of Steps
Mass mean diameter (d_g)	0.05 – 1.0 μm	0.05 μm	20
Geometric standard deviation	1.1 – 3.0	0.1	20
Real part of index of refraction	1.3 – 1.8	0.05	11
Imaginary part of index of refraction	0.000 – 0.200	0.005	41
Density	1.0 – 2.0 g/cm^3	0.05 g/cm^3	21

Figure 1 plots the variability in α_M for the above analysis using the various combinations of d_g, σ_g, n and k listed in Table 1 at a single aerosol density, $\rho = 1.3 \text{g/m}^3$. Careful examination of Figure 1 indicates that, in the ranges examined, changes in the real part of the index of refraction and mass mean diameter have a larger effect on in α_M than changes in the geometric standard deviation or imaginary part of index of refraction. This effect has also been reported by others.^{14,15,18}

Figure 1. Variation in theoretical scattering efficiency (α_M in m^2/g) calculated from Mie theory for variations in mass mean diameter (d_g in μm), geometric standard deviation (σ_g), real part of imaginary index of refraction (n), and imaginary part of index of refraction (k). Aerosol density is $1.3g/m^3$ for all plots. A: $n=1.5$ and $k=0.02$, B: $\sigma_g=1.8$ and $k=0.02$, C: $\sigma_g=1.8$ and $n=1.5$, D: $d_g=0.4$ and $k=0.02$, E: $d_g=0.4$ and $n=1.5$, and F: $d_g=0.4$ and $\sigma_g=1.8$.

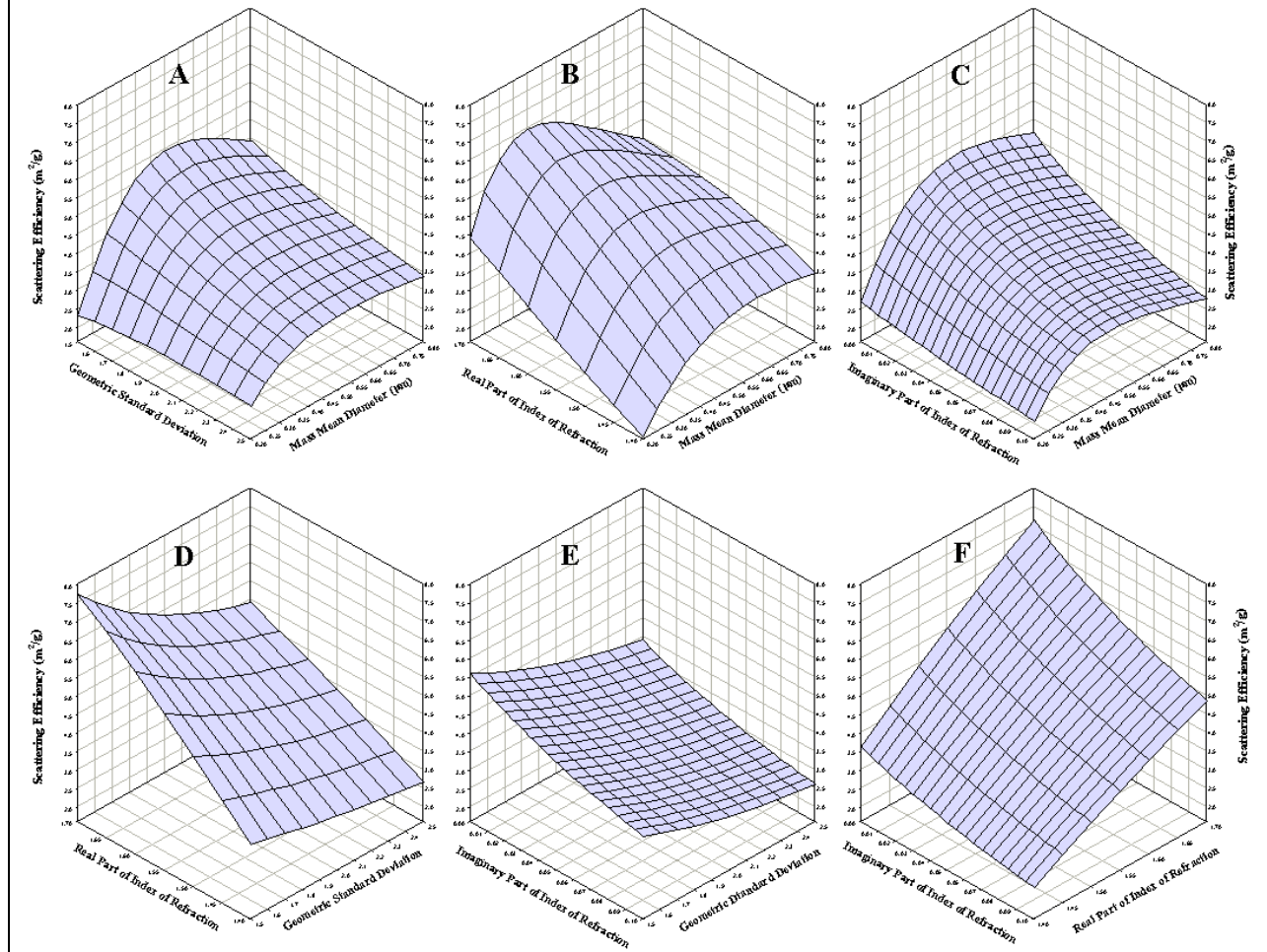
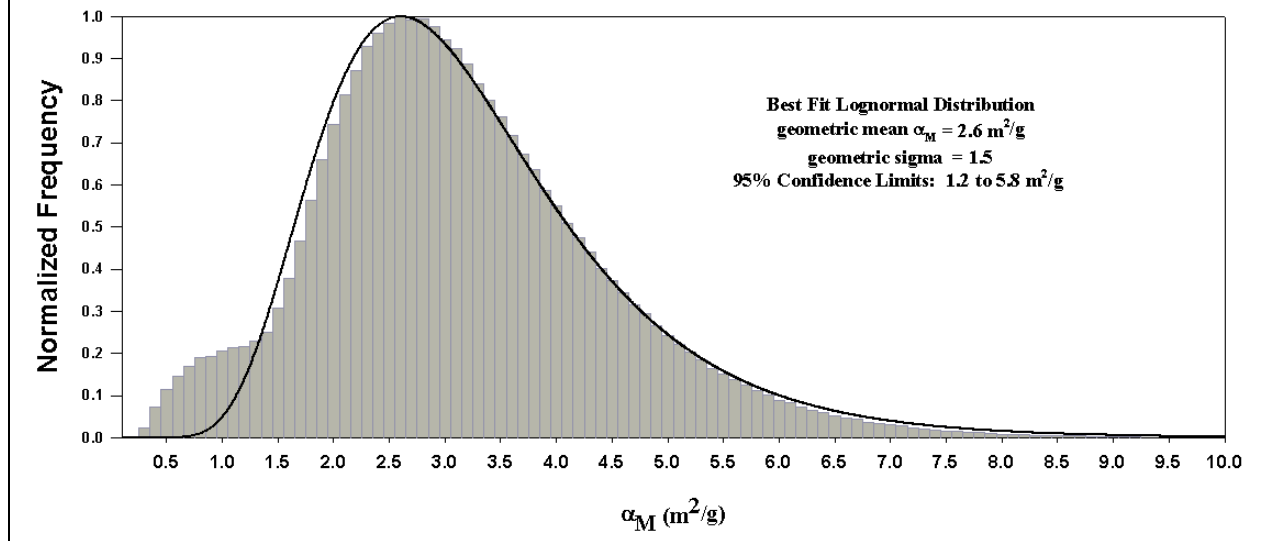


Figure 2 plots the normalized frequency distribution of α_M (in $0.1m^2/g$ bins) calculated from data generated for Figure 1 and allowing aerosol density to vary from $\rho = 1.0$ to $\rho = 2.0g/cm^3$ in $0.1g/cm^3$ bins. The resulting distribution can be reasonably fit by a lognormal distribution with geometric mean $\alpha_M=2.6m^2/g$ and geometric standard deviation=1.5. This results in a 95% confidence interval of 1.2 to $5.8m^2/g$ for α_M . This means, that assuming the $PM_{2.5}$ aerosol parameters vary independently and uniformly throughout the ranges discussed above, the output of a light scattering photometer indicating $26\mu g/m^3$ calibrated to a mean $PM_{2.5}$ aerosol α_M of $2.6m^2/g$, the actual $PM_{2.5}$ mass concentration has a 95% probability of being between $12\mu g/m^3$ and $58\mu g/m^3$, which is -54% to $+123\%$ of the assumed correct value.

Figure 2. Normalized frequency distribution of scattering mass ratio (α_m) for range of parameters discussed in text.



INCORPORATION OF CORRELATIONS IN AEROSOL PARAMETERS

In reality, aerosol parameters are not independent. An aerosol model was developed in an attempt to realistically account for the effect of correlations between parameters that may minimize the range of α_M for actual $\text{PM}_{2.5}$ aerosols.

PM_{2.5} Aerosol Model

Following White *et al.*⁴⁹ and McMurry *et al.*,²⁴ the $\text{PM}_{2.5}$ aerosol is considered to be composed of two separate externally mixed haze and dust fractions. The haze is considered to be an internal mixture of sulfate, nitrate, organic and light absorbing carbon (LAC). An internal mixture is considered to be one in which all the aerosol of a given size consists of a homogeneous combination of the species. The $\text{PM}_{2.5}$ dust fraction is composed of crustal material, referred to as fine soil. When computing bulk aerosol scattering properties, the microscopic structure of the aerosol (that is, the extent of internal or external mixing) is found to be relatively unimportant, so that the assumption of internally vs. externally mixed particles does not have much impact on the predicted results. This insensitivity has been demonstrated by a number of authors.^{17-25,50}

Aerosol data from 60 sites in the Interagency Monitoring of Protected Visual Environments (IMPROVE) visual air quality monitoring program were used to calculate daily $\text{PM}_{2.5}$ aerosol species for the period 1988–1999. Methods for apportionment of measured mass to the various aerosol species are explored in detail by Malm *et al.*,^{51,52} and Eldred *et al.*⁵³ The resulting data set contained 44,946 days of gravimetric $\text{PM}_{2.5}$ mass and speciated aerosol data from 58 remote Class I monitoring sites and two urban areas, Washington, D.C. and South Lake Tahoe, Ca.

Nitrate Loss

The sum of the five primary aerosol species: sulfates, nitrates, organics, light-absorbing carbon and soil should provide a reasonable estimate of the PM_{2.5} mass measured on the teflon filter media used to measure gravimetric PM_{2.5} mass. However, a significant fraction of the nitrate particles can volatilize from the teflon filter during collection and is not measured by gravimetric analysis.⁵⁴ The amount of nitrate loss varies from less than 10% to greater than 90% depending on the time of year, ambient temperature, sampling duration and aerosol chemistry. For this analysis, it was assumed that on average, 50% of the nitrate is lost from the teflon filter. Bergin *et al.*⁵⁵ report an analysis of the loss of nitrate aerosol due to heating of the inlet of a size cut integrating nephelometer. They indicate that 20%-50% of the nitrate is lost due to this heating. Thus, assuming 50% of the nitrate is lost from the teflon filter essentially matches the loss of nitrate due to the heated inlet of the nephelometers that is required to bring the sampling chamber relative humidity down to 40%.

In addition to the loss of nitrate, the sum of the PM_{2.5} species usually underestimates the measured gravimetric PM_{2.5} mass. The difference between the measured and reconstructed dry PM_{2.5} mass is denoted as unexplained mass. Gravimetric weighing occurs in a laboratory held at a relative humidity of 40%±5%. Even at this low relative humidity, the aerosol can have significant water associated with it. This unexplained mass is thought to be residual water on the aerosol at the time the filter is weighed.⁵⁶

Residual Water Mass Model

In the absence of detailed size resolved speciated aerosol data, semi-empirical growth curves derived for “typical” atmospheric aerosols have been used for reasonable estimates of the water mass associated with hydrated aerosols. Sloane²¹ has discussed the following semi-empirical growth curve, which has a theoretical foundation.⁵⁷

Equation 2.

$$\left(\frac{D}{D_o}\right)^3 = 1 + F_s \rho_{dry} EH \left(\frac{RH}{1 - RH}\right).$$

where:

D is the diameter at a relative humidity, RH ; D_o is the dry particle diameter; F_s is the soluble fraction of dry mass (0.0 to 1.0); and ρ_{dry} is the average density of the dry aerosol.

Equation 2 assumes that all of the species in the soluble fraction absorb the same amount of water. The composite function EH , which is generally determined empirically for “typical” mixtures and which varies with composition and RH , is defined by:

Equation 3.

$$EH = \langle i \rangle \langle \varepsilon \rangle \frac{MW_w}{\langle MW_s \rangle}$$

where:

i is the van't Hoff factor, which accounts for dissolution of ionic species into ions in solution; ε is the dissolved fraction of the aerosol mass; $\langle MW_s \rangle$ is the average molecular weight of solute; and MW_w is the molecular weight of water. Table 2 shows values for $EH(RH)$ as used by Sloane,²¹ Lowenthal *et al.*²³ and Malm and Kreidenweis.²⁵ Malm and Kreidenweis have shown that using $EH=0.35$ at $RH=40\%$, results in the best fit with a more rigorous model for internally mixed aerosol and will be used in this analysis. Thus, employing solid geometry and equation 2 with $EH=0.35$, and $RH=40\%$, the water mass associated with the soluble species can be estimated as:

Equation 4.

$$[\text{Water}]_{RH=40\%} = 0.23 F_s [\text{RCFH}]_{\text{DryHaze}}$$

$[\text{RCFH}]_{\text{DryHaze}}$ is the dry $\text{PM}_{2.5}$ haze mass on the teflon filter:

Equation 5.

$$[\text{RCFH}]_{\text{DryHaze}} = [\text{Sulfate}] + 0.5[\text{Nitrate}] + [\text{Organic}] + [\text{LAC}]$$

The soluble mass fraction (F_s) is considered to contain all the sulfate, nitrate that remains on the teflon filter, and some fraction (f_{oc}) of the organic aerosol:

Equation 6.

$$F_s = ([\text{Sulfate}] + 0.5[\text{Nitrate}] + f_{oc}[\text{Organic}]) / [\text{RCFH}]_{\text{DryHaze}}$$

The remaining fraction ($1-f_{oc}$) of organic aerosol and all the LAC is considered to be insoluble. The wet haze mass then is:

Equation 7.

$$[\text{RCFH}]_{\text{WetHaze}} = [\text{RCFH}]_{\text{DryHaze}} + [\text{Water}]_{RH=40\%}$$

Table 2. Thermodynamic functions for particle growth: $(\langle i \rangle \langle E_h \rangle MW_w) / \langle MW_s \rangle$.

Relative Humidity %	30	40	50	60	70	80	90
Continental Urban Sloane ²¹	0.24	0.24	0.30	0.54	0.67	0.58	0.46
Typical Urban Sloane ²¹	0.20	0.40	0.60	0.70	0.75	0.65	0.60
Lowenthal et al. ²³	0.09	0.12	0.13	0.13	0.17	0.27	0.23
Malm and Kreidenweis ²⁵	0.09	0.35	0.35	0.35	0.32	0.27	0.23

A major uncertainty exists as to the solubility of PM_{2.5} organic species.⁵⁸ To see if a reasonably good average value for the soluble fraction of organics could be determined from the IMPROVE data set, the average wet reconstructed mass [RCFM]_{wet} and gravimetric PM_{2.5} mass for all 60 IMPROVE sites were calculated. [Water]_{RH=40%} was calculated with equations 3-6 allowing the soluble fraction of organic mass to vary from $foc=0.0$ to $foc=1.0$. The best fit occurred with a soluble organic fraction $foc=0.5$.

Volume Average Bulk Aerosol Parameters

Using density and index of refraction parameters listed in Table 3 for each species calculated with the above model, the volume average,^{17,34} wet and dry bulk PM_{2.5} haze aerosol density, real and imaginary index of refraction were calculated for all 44,946 aerosol days in the IMPROVE data set. Figure 3 plots the normalized joint frequency distributions for all combinations of ρ , n , and k for both the dry and wet PM_{2.5} haze aerosol. The data in Figure 3 are combined to generate a joint probability distribution of (ρ, n, k) for the PM_{2.5} haze aerosol.

Table 3. Density and index of refraction for PM_{2.5} haze and PM_{2.5} dust aerosol species.

Species	Density g/cm ³	Index of Refraction	References
Ammonium Sulfate	1.76	1.53 ± 0.00	Tang ⁵⁰
Ammonium Nitrate	1.725	1.55 ± 0.00	Tang ⁵⁰
Organic	1.0	1.50 ± 0.00	McMurry et al. ²⁴
LAC (soot A)	2.0	1.95 ± 0.66	Fuller et al. ⁵⁹
Water	1.0	1.335 ± 0.00	McMurry et al. ²⁴
PM _{2.5} Dust	2.3	1.53 ± 0.0055	Diner et al. ⁴¹

Aerosol Model Assumptions

It bears repeating the model assumptions that this joint probability distribution for PM_{2.5} haze aerosol physical parameters (ρ, n, k) rests on:

1. The PM_{2.5} aerosol can be modeled as two externally mixed fractions, haze and dust.
2. The haze fraction is internally mixed.
3. On average 50% nitrate remains on teflon filter.
4. On average 50% of organic is soluble.
5. The filters are weighed at an average laboratory relative humidity of $RH=40\%$.
6. The water mass associated at $RH=40\%$ can be adequately modeled with the semi-empirical growth function and a constant $EH=0.35$ for all soluble species.
7. Volume averaging is appropriate for calculating average aerosol density, the real and the imaginary part of index of refraction.

PM_{2.5} Haze Aerosol Size Distribution

No easily accessible large data set similar to the IMPROVE speciated aerosol data exists for measured mass mean diameters and geometric standard deviations to make anything other than a reasonable estimate as to their joint frequency distribution. Therefore, a best guess was made using data from Malm and Pitchford.⁶⁰ Figure 4 plots the joint frequency distribution of mass mean diameter and geometric standard deviation that will be used to estimate α_M for the PM_{2.5} haze aerosol calculated from the IMPROVE data set. The aerosol parameters (d_g, σ_g) were assumed to be lognormally distributed with a geometric mean and standard deviation of $0.4\mu\text{m}$ and 1.5 for d_g and 1.8 and 1.25 for σ_g . Because no good information exists to determine any possible correlations with PM_{2.5} haze aerosol physical parameters (ρ, n, k), the joint frequency distribution (d_g, σ_g) is assumed to be independent from the joint frequency distribution (ρ, n, k).

Figure 3. Normalized joint frequency distributions of aerosol physical parameters (ρ, n, k) for IMPROVE data set dry and wet PM_{2.5} haze aerosol. Wet aerosol calculated with semi-empirical water uptake model at $RH=40\%$.

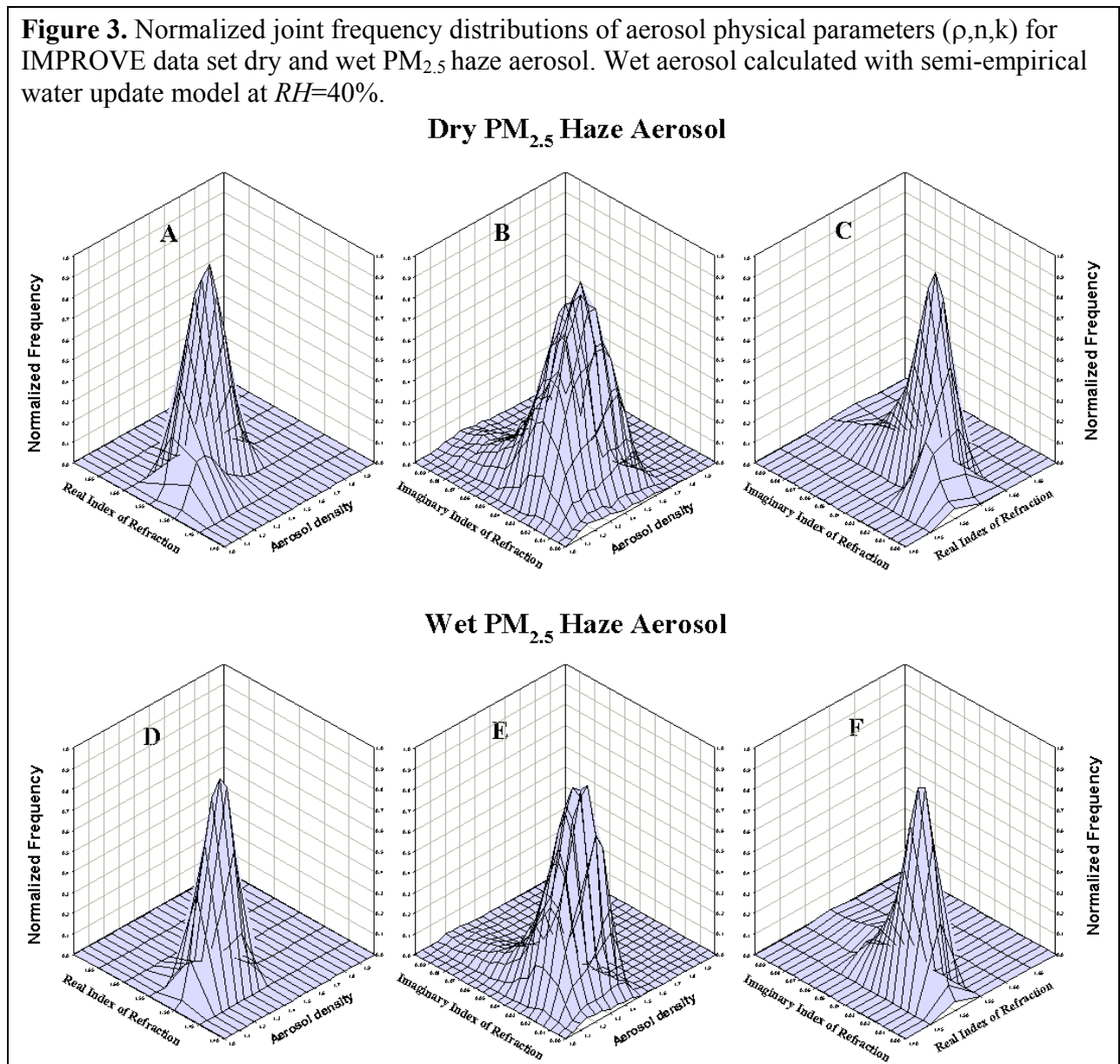
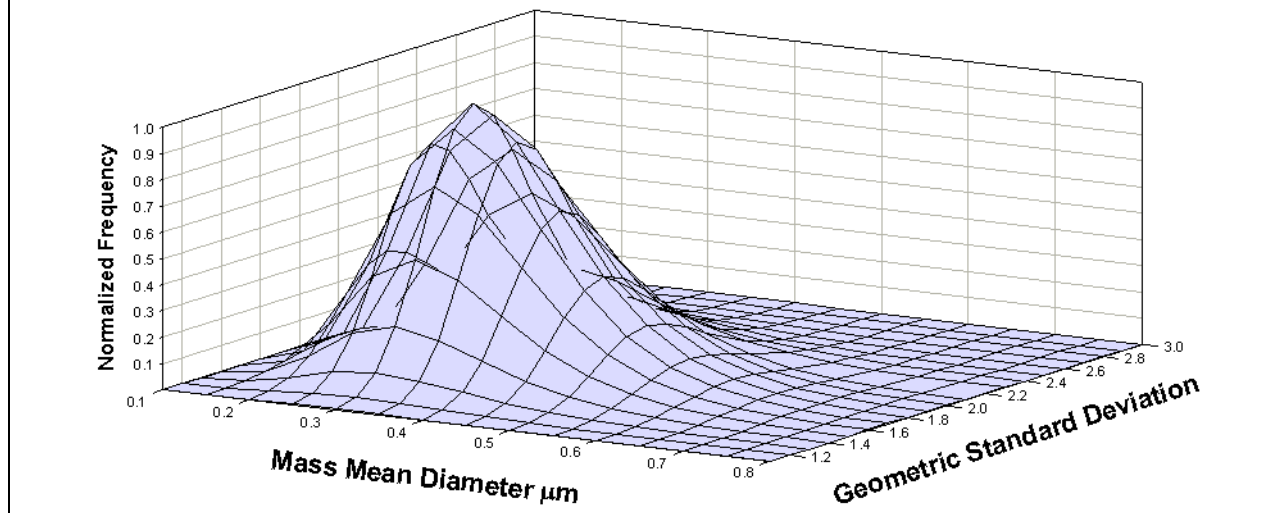


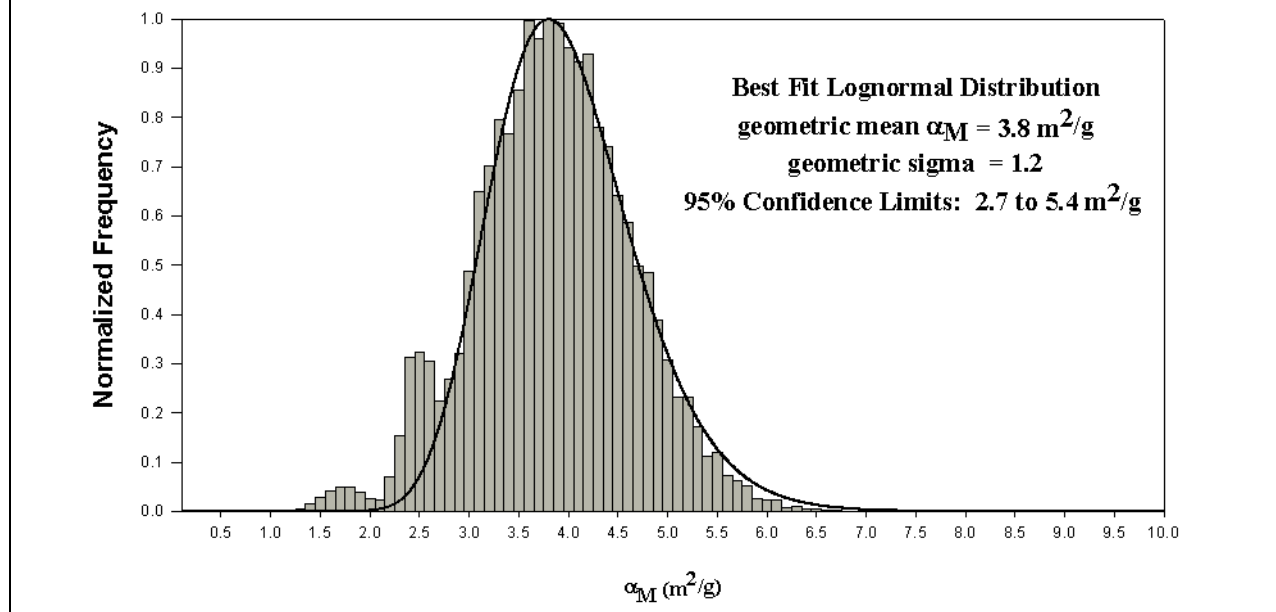
Figure 4. Normalized joint frequency distribution of PM_{2.5} haze aerosol mass mean diameter and geometric standard deviation used in aerosol model.



Joint Distributions of PM_{2.5} Haze Aerosol α_M

The frequency distribution of scattering efficiencies calculated assuming independent uniform distributions of d_g , σ_g , ρ , n , and k plotted in Figure 2 was weighted by the joint probability calculated from the frequency distributions for (ρ, n, k) and (d_g, σ_g) . Figure 5 plots the resulting frequency distribution of α_M using the above PM_{2.5} haze aerosol model. The resulting distribution of calculated α_M can be best fit as lognormal distribution with a geometric mean $\alpha_M = 3.8 \text{ m}^2/\text{g}$ and a geometric standard deviation of $1.2 \text{ m}^2/\text{g}$. The 95% confidence interval is then $2.7 \text{ m}^2/\text{g}$ to $5.4 \text{ m}^2/\text{g}$ for the PM_{2.5} haze fraction of PM_{2.5} aerosol, which is a considerably reduced range than when assuming a uniform and independent variation of the PM_{2.5} aerosol physical parameters, d_g , σ_g , ρ , n and k .

Figure 5. Normalized frequency distribution of calculated scattering mass ratio (α_m) for a the calculated joint frequency of d_g , σ_g , ρ , n , and k from $PM_{2.5}$ haze aerosol model.



Incorporation of $PM_{2.5}$ Dust Aerosol

The final distribution of α_M for the IMPROVE data set is calculated by determining the distribution of haze and dust fractions for the $PM_{2.5}$ aerosol and volume averaging the scattering efficiencies of the two fractions. Figure 6 plots the $PM_{2.5}$ dust mass fraction (%) frequency distribution for the IMPROVE data set. Following Diner *et al.*,⁴¹ the $PM_{2.5}$ dust fraction is considered to have constant values of: $d_g=0.95\mu\text{m}$, $\sigma_g=2.6$, $\rho=2.3\text{g/m}^3$, $n=1.53$, and $k=0.0055$ at 550nm. Mie theory calculations for this $PM_{2.5}$ dust model results in $\alpha_M=2.0$, which is slightly lower than the $PM_{2.5}$ dust scattering efficiencies of 2.3–3.1 m^2/g reported by White *et al.*,⁴⁹ and McMurry *et al.*²⁴ The $PM_{2.5}$ haze α_M distribution in Figure 5 is volume averaged with the $PM_{2.5}$ dust distribution. The resulting frequency distribution (Figure 7) is the final estimate of the wet ($RH=40\%$) $PM_{2.5}$ aerosol scattering efficiency distribution for the IMPROVE aerosol data set. The resulting distribution of calculated α_M can be best fit as lognormal distribution with a geometric mean $\alpha_M=3.7\text{m}^2/\text{g}$ and a geometric standard deviation of 1.2 m^2/g . The 95% confidence interval is then 2.6 m^2/g to 5.3 m^2/g for the $PM_{2.5}$ haze fraction of $PM_{2.5}$ aerosol. This slight change in mean α_M is expected since, on average, $PM_{2.5}$ dust is a small fraction of the $PM_{2.5}$ mass in the IMPROVE data set. A recent analysis of a large data set of aerosol light scattering measured by a heated integrating nephelometer and $PM_{2.5}$ gravimetric mass from the 1995 Integrated Monitoring Study in the San Joaquin Valley, Ca. resulted in an average $\alpha_M=3.67 \pm 0.05\text{m}^2/\text{g}$, and a range in α_M from 2.7 m^2/g to 4.3 m^2/g for various aerosol species.⁶¹

This analysis means, that with the described $PM_{2.5}$ aerosol model, when the output of a light scattering photometer calibrated to a mean $PM_{2.5}$ aerosol α_M of 3.7 m^2/g indicates 15 $\mu\text{g}/\text{m}^3$, the actual $PM_{2.5}$ mass concentration has a 95% probability of being between 10.5 $\mu\text{g}/\text{m}^3$ (-30%) and 21 $\mu\text{g}/\text{m}^3$ (+40%). If the $PM_{2.5}$ aerosol is reasonably represented by the described model, an

irreducible uncertainty of approximately $\pm 40\%$ will exist in $PM_{2.5}$ mass from light scattering measurements.

Figure 6. $PM_{2.5}$ dust mass fraction frequency of occurrence for IMPROVE aerosol data set.

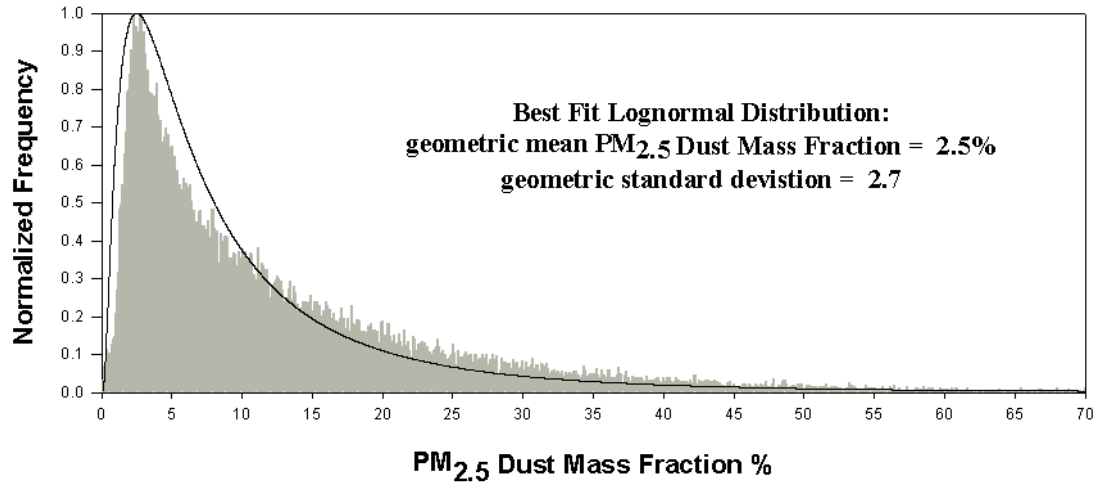
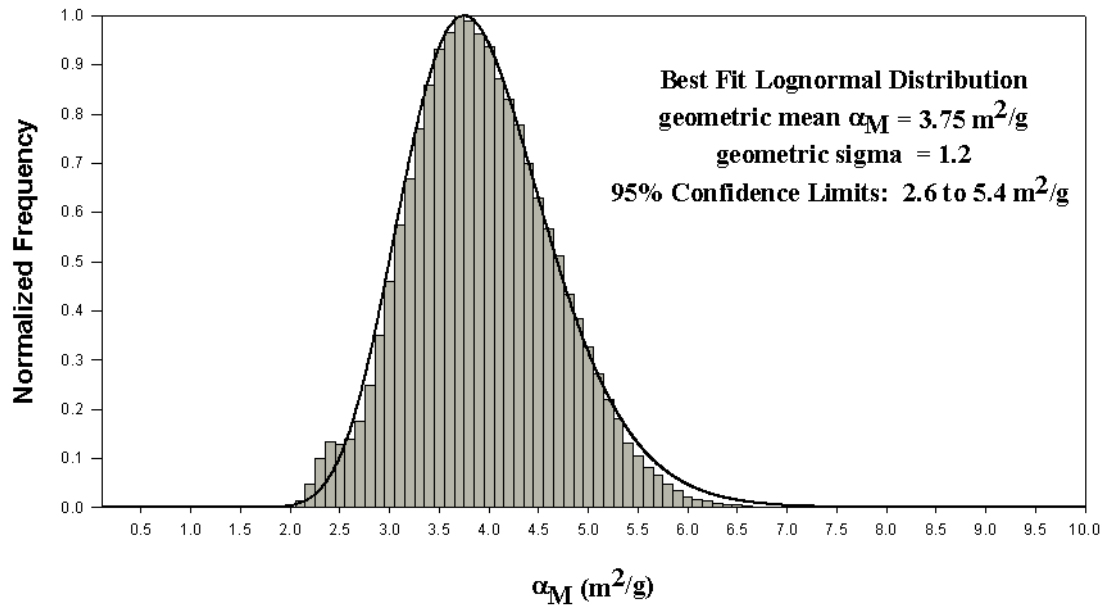


Figure 7. Best estimate of normalized frequency distribution of calculated scattering mass ratio (α_m) for a the calculated joint frequency of $d_g, \sigma_g, \rho, n,$ and k for $PM_{2.5}$ aerosol (haze + fine dust) from IMPROVE data.



NEPHELOMETRY AND LIGHT SCATTERING PHOTOMETRY

Nephelometry is a mature science dating back 50 years with well understood design philosophies and inherent limitations.⁶² Integrating nephelometers have proven to be capable of making highly accurate, precise continuous measurements of the aerosol scattering coefficient. In addition, nephelometers are very portable, rugged, requiring low maintenance and of moderate cost when compared to filter based aerosol samplers. The signal output by an integrating nephelometer is proportional to:

Equation 8.

$$2 \pi \int_{\lambda} \int_{\varphi} B(\varphi, \lambda) \sin(\varphi) d\varphi R(\lambda) d\lambda$$

where:

$B(\varphi, \lambda)$ is the volume scattering function of the aerosol and gas, $R(\lambda)$ is the spectral response function of the instrument, integration over λ is for all wavelengths the nephelometer is sensitive to, and integration over φ is over the integration angle of the instrument.

The volume scattering function, both of the calibrating gas and aerosol to be measured, is a function of wavelength and scattering angle. Thus, the measured scattering coefficient depends on the weighted average of the instrument response of both the aerosol and Rayleigh calibration gas or calibration aerosol.

In principle, it would be best to calibrate a nephelometer with laboratory aerosols of known physical parameters that closely approximated those of the ambient aerosol to be monitored. This method has been attempted by several authors⁶²⁻⁶⁴ with reasonable results. However, away from a laboratory, these procedures are very difficult. Thus, integrating nephelometers are typically calibrated with a dense inert high refractive index gas with known scattering properties. Models of the response of integrating nephelometers show that for the $PM_{2.5}$ aerosol, calibrating with a Rayleigh gas results in less than 5% error in the measured aerosol scattering coefficient, Figure 8.^{62,64-66} This demonstrably small error in measured $PM_{2.5}$ aerosol scattering coefficient, indicates that properly operated integrating nephelometers will add only a few percent to the large uncertainty in $PM_{2.5}$ mass estimates from scattering measurements that comes from varying aerosol properties.

Light scattering photometers do not integrate the scattered signal over a large scattering angle φ . The detectors of these instruments typically only view a portion of the scattering volume. Currently commercially available light scattering photometers fall into two basic geometries: 1) Forward Scattering - scattering angle range 45° - 50° to 90° - 95° (Mie DataRam, Met One Gt-640, R&P DustLite 3000), and 2) Orthogonal Scattering – scattering angle range 87° to 90° (TSI DustTrak, Grimm DustCheck). These systems are typically calibrated with a standard test aerosol, ISO 12103 – A1 (Arizona Test Dust). This aerosol has the following physical properties: $r=2.6g/m^3$, index of refraction = $1.5 \pm 0.00i$, $d_g=2\mu m$ to $3\mu m$, and $\sigma_g=2.5$. These are all significantly different from $PM_{2.5}$ aerosols. Using the standard factory calibrations with these systems will lead to a significant over estimation of $PM_{2.5}$ mass because the scattering efficiency

of Arizona Test Dust is about 50% of the $PM_{2.5}$ aerosol α_M . Table 4 lists these values at published wavelengths of these systems. $PM_{2.5}$ aerosol scatters about twice as much light per unit mass as the coarse Arizona Test Dust, thus $1\mu g/m^3$ of $PM_{2.5}$ scatters as much as $2\mu g/m^3$ Arizona Test Dust. Therefore, the output of the instrument will be about 2 times higher than reality varying with the variability of $PM_{2.5}$ aerosol α_M as discussed previously.

Figure 8. Modeled error in aerosol scattering coefficient for various integrating nephelometers at their published effective wavelengths for a lognormal $PM_{2.5}$ aerosol distribution as a function of mass mean diameter. The model includes Rayleigh gas corrected truncation effects and spectral response of instruments.⁶⁵

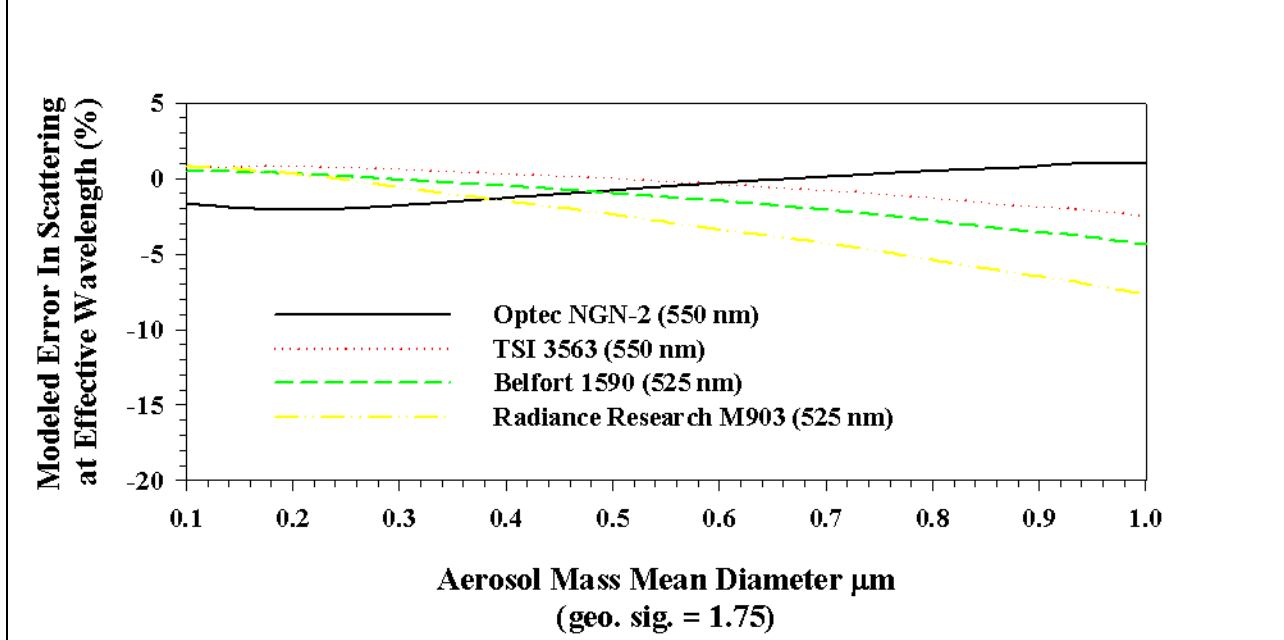


Table 4. Mie calculated scattering efficiencies for Arizona Test Dust and $PM_{2.5}$ aerosol at various wavelengths of commercial light scattering photometers. Ratio is the mass error associated with calibrations by Arizona Test Dust due to significant differences in α_M .

Light Scattering Photometer	Wavelength	$PM_{2.5}$ Aerosol α_M (m^2/g)	AZ Test Dust α_M (m^2/g)	Ratio: $PM_{2.5} / AZ$ Test Dust
Grimm DustCheck Met One GT-640 TSI DustTrak	780 nm	2.5	1.07	2.3
Mie DataRam R&P Dustlite	880 nm	1.9	1.04	1.8

In addition to errors associated with the different scattering efficiencies, the scattering phase functions are significantly different for Rayleigh gas, $PM_{2.5}$ aerosol, and Arizona Test Dust. Figure 9 plots the normalized phase functions for Rayleigh gas, $0.2\mu m$, $0.8\mu m$ $PM_{2.5}$ aerosol distributions and Arizona Test Dust. The output of a nephelometer or light scattering photometer will be proportional to the area under the phase function curves for the measured aerosol in the

detection angle of the instrument. The calibrated output will be proportional to the ratio of the area under the phase function curves of measured aerosol and calibration gas or aerosol in the detection angle of the instrument. The estimated error for integrating nephelometers (Figure 8) is relatively low for PM_{2.5} aerosols because the area under the phase functions of the PM_{2.5} aerosol and calibration gas are nearly equal. For light scattering photometers that only detect a small fraction of the scattered light, this is not true. Figure 10 plots the error associated with using Arizona Test Dust as a calibration aerosol and measuring PM_{2.5} aerosols. Only for the largest PM_{2.5} aerosol d_g , does the error approach reasonable levels (20%) as the phase functions become similar in the detector scattering angles.

CONCLUSIONS

The intensity of scattered radiation by a polydisperse lognormal aerosol distribution is not simply linearly related to dry aerosol mass concentration, but rather a function of the size distribution parameters, aerosol density and index of refraction. Current integrating nephelometers calibrated with Rayleigh gases, are accurate and precise enough to make excellent measurements of the PM_{2.5} aerosol scattering coefficient $bsp_{2.5}$. Field studies indicate a good correlation between $bsp_{2.5}$ and gravimetric PM_{2.5} aerosol mass. Analyses using Mie theory and reasonable estimates of the range of aerosol physical parameters (ρ, n, k) and size distribution parameters (d_g, σ_g) show that this correlation should be expected. However, the analyses also indicate that an estimate of aerosol mass by nephelometry will have an irreducible uncertainty of approximately $\pm 30\%$ - 40% . This uncertainty is directly attributable to the natural variability of PM_{2.5} aerosol parameters, independent of how good a nephelometer or light scattering photometer can be made to perform.

In addition to this inherent uncertainty, light scattering photometers used with standard calibrations employing Arizona Test Dust will significantly overestimate the actual PM_{2.5} mass concentrations due to significant differences in the phase functions and scattering efficiencies between the calibration and ambient PM_{2.5} aerosol. These type of instruments must be calibrated with simultaneous gravimetric measurements of the ambient PM_{2.5} aerosol to calculate an appropriate calibration constant.

Figure 9. Normalized scattering phase functions for a Rayleigh calibration gas, 0.2 μm & 0.8 μm aerosol size distributions and Arizona Test Dust used to calibrate forward scattering and orthogonal photometers. Detector acceptance angles for various nephelometers and light scattering photometers are indicated.

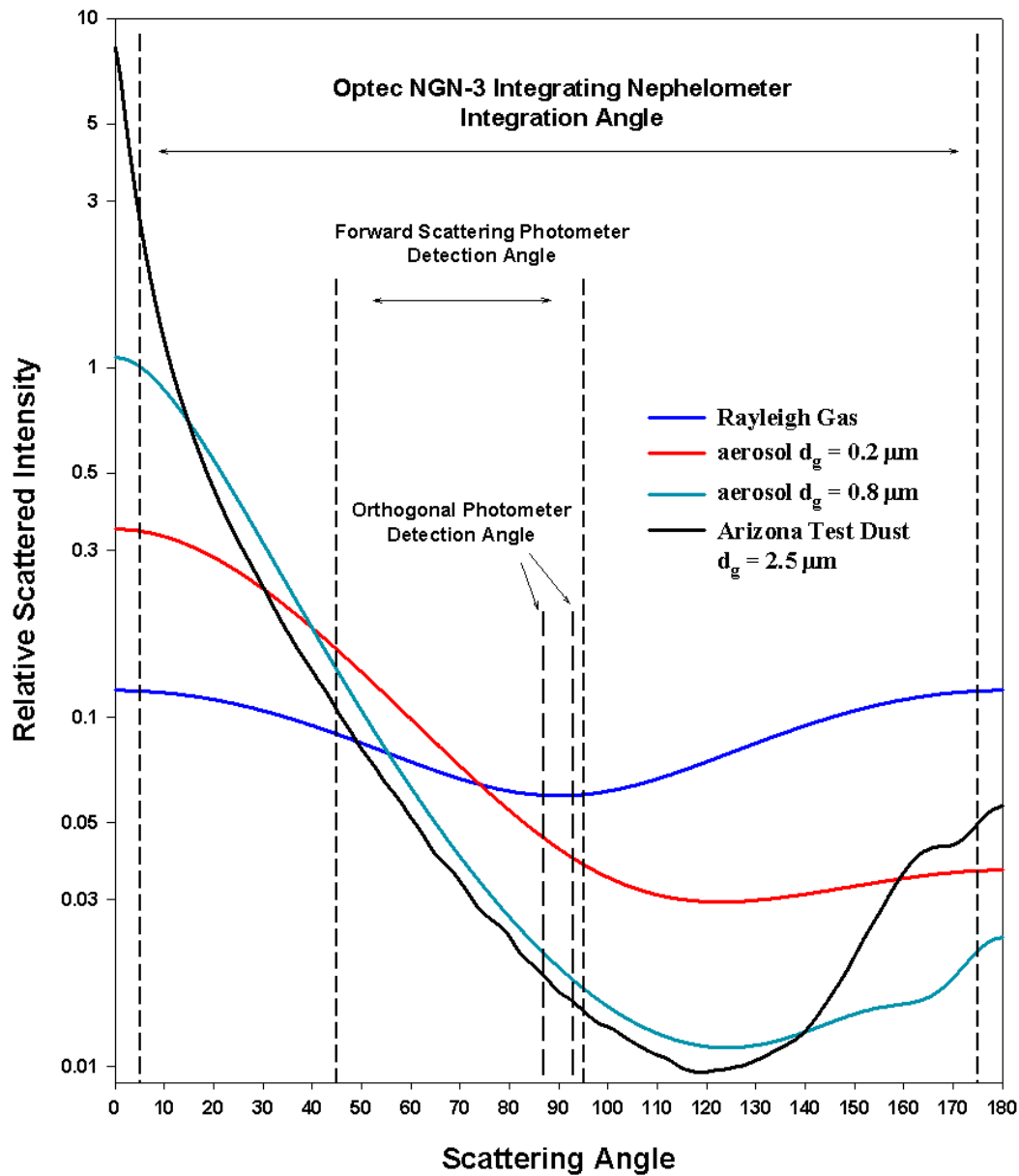
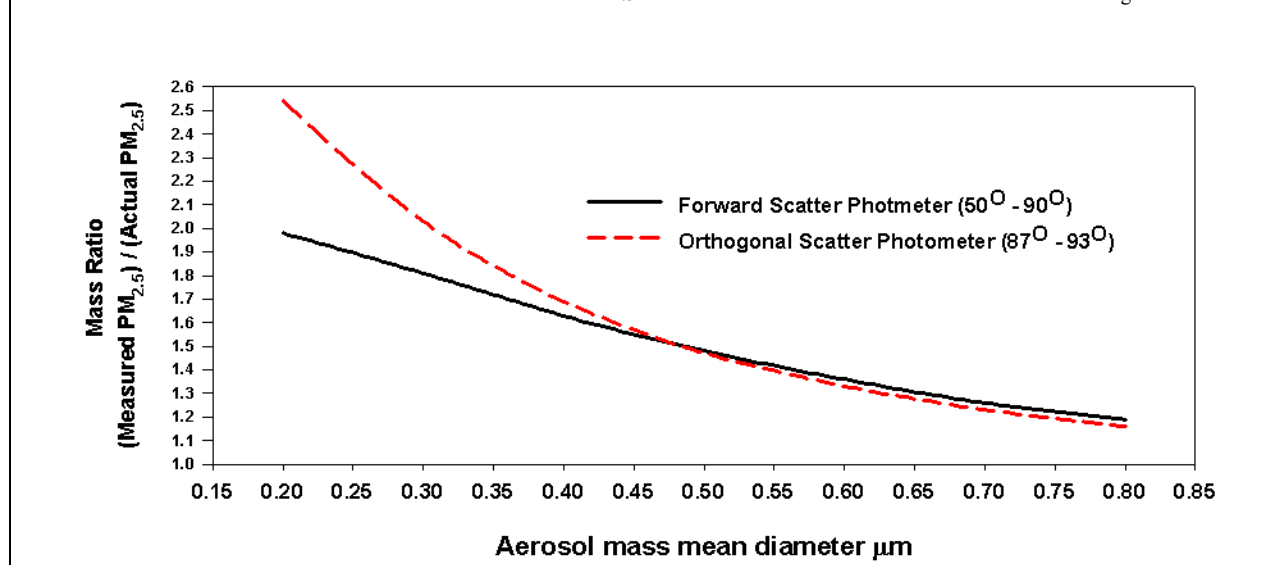


Figure 10. Mie calculated error in measured PM_{2.5} mass for forward scatter and orthogonal light scattering photometers calibrated with Arizona Test Dust due to differences in normalized phase functions between Arizona Test Dust and PM_{2.5} aerosol distributions with indicated d_g .



REFERENCES

1. Robinson, E. The effects of air pollution on visibility. In *Air Pollution*, Vol. 1, 2nd edition, A.C. Stern, Ed.; Academic Press, NY 1968; pp 349-99.
2. Charlson, R.J.; Ahlquist, N.C.; Horvath, H. On the generality of correlation of atmospheric aerosol mass concentration and light scatter. *Atmos. Environ.* **1968**, *2*, 455-464.
3. Ahlquist, N.C.; Charlson, R.J. A new instrument for measuring the visual quality of air. *JAPCA* **1967**, *17*, 467-469.
4. Charlson, R.J. Atmospheric visibility related to aerosol mass concentration: A review. *Environ. Sci. Technol* **1969**, *3*, 913-918.
5. Ettinger, H.J.; Royer, G.W. Visibility and mass concentration in non-urban environment. *JAPCA* **1972**, *22*, 108-111.
6. Kretzschmar, J.G. Comparison between three different methods for measuring suspended particulates in air. *Atmos. Environ.* **1975**, *9*, 931-934.
7. Waggoner, A.P.; Weiss, R.E. Comparison of fine particle mass concentration and light scattering extinction in ambient aerosol. *Atmos. Environ.* **1980**, *14*, 623-626.
8. Dzubay, T.G.; Stevens, R.K.; Lewis, C.W.; Hern, D.H.; Courtney, W.J.; Tesch, J.W.; Mason, M.A. Visibility and aerosol composition in Houston. *Environ. Sci. Technol.* **1982**, *16*, 514-525.
9. Willeke, K.; Whitby, K.T. Atmospheric aerosols: size distribution interpretation. *JAPCA* **1975**, *25*, 529-534.
10. Whitby, K.T. The physical characteristics of sulfur aerosols. *Atmos. Environ.* **1978**, *12*, 135-139.
11. Waggoner, A.P.; Weiss, R.E.; Ahlquist, N.C.; Covert, D.S.; Will, S.; Charlson, R.J. Optical characteristics of Atmospheric aerosols. *Atmos. Environ.* **1981**, *15*, 1891-1909.
12. White, W.H. The components of atmospheric light extinction: a survey of ground level budgets. *Atmos. Environ.* **1990a**; *24a*, 2673-2679.

13. White, W.H. Appendix H Dry Fine-Particle Scattering Efficiencies: In - Visibility: Existing and historical conditions – Causes and effects. *State Sci. and Technol. Rep. 24*, Natl. Acid Precip. Assess. Program, Washington, D.C., 1990b; p 24-H1.
14. Willeke, K.; Brockman, J.E. Extinction coefficient for multimodal atmospheric particle size distributions. *Atmos. Environ.* **1977**, *11*, 995-999.
15. Lewis, C.W. On the proportionality of fine mass concentration and extinction coefficient for bimodal size distributions. *Atmos. Environ.* **1981**, *15*, 2639-2646.
16. Mie, G. Beitrage zur Optik trueber Medien, speziell kolloidaler Metallosungen. *Ann. Phys.*, **1908**, *25*, 377-445.
17. Ouimette, J.R.; Flagan, R.C. The extinction coefficient of multi-component aerosols. *Atmos. Environ.* **1982**, *16*, 2405-2419.
18. Hasan, H.; Dzubay, T.G. Apportioning light extinction coefficients to chemical species in atmospheric aerosol. *Atmos. Environ.* **1983**, *17*, 1573-1581.
19. Sloane, C.S. Optical properties of aerosols – comparison of measurements with model calculations. *Atmos. Environ.* **1983**, *17*, 409-416.
20. Sloane, C.S. Optical properties of aerosols of mixed composition. *Atmos. Environ.* **1984**, *18*, 871-878.
21. Sloane, C.S. Effect of composition on aerosol light scattering efficiencies. *Atmos. Environ.* **1986**, *20*, 1025-1037.
22. White, W.H. On the theoretical and empirical basis for apportioning extinction by aerosols: A critical review. *Atmos. Environ.* **1986**, *20*, 1659-1672.
23. Lowenthal, D.H.; Rogers, C.F.; Saxena, O.; Watson, J.G.; Chow, J.C. Sensitivity of estimated light extinction coefficients to model assumptions and measurement errors. *Atmos. Environ.* **1995**, *29*, 751-766.
24. McMurry, P.H.; Dick, W.D.; Saxena, P.; Musarra, S. Mie theory evaluation of species contributions to visibility reduction in the smoky mountains: results from the 1995 SEAVS study. In *Visual Air Quality: Aerosols and Global Radiation Balance*, Air and Waste Management Association, Pittsburgh, 1997; pp 394-399.
25. Malm, W.C.; Kreidenweis, S.M. The effects of models of aerosol hygroscopicity on the apportionment of extinction. *Atmos. Environ.* **1997**, *31*, 1965-1976.
26. U.S.EPA National ambient air quality standards for particulate matter – final rule. 40 CFR Part 50. *Federal Register* 62(138): 38651-38760. July 18, 1997.
27. U.S.EPA Guidance for using continuous monitors in PM_{2.5} monitoring networks. *OAQPS EPA-454/R-98-012*, May 1998.
28. Chow, J.C.; Watson, J.G.; Lowenthal, D.H.; Hackney, R.; Magliano, K.; Lehrman, D.; Smith, T. Temporal variations on PM_{2.5}, PM₁₀, and gaseous precursors during the 1995 integrated monitoring study in central California. *J. Air & Waste Manage. Assoc.* **1999**, *49*, PM-16-24.
29. VanCurren, T. Spatial factors influencing winter primary particle sampling and interpretation. *J. Air & Waste Manage. Assoc.* **1999**, *49*, PM-3-15.
30. Moore, T.; Fitch, M.; Adlhoch, J.; Lahm, P. Effects of filtering out rapid transitory changes in optical visibility data: extrapolating the results of a case study analysis from the Grand Canyon National Park to selected class I areas in the western United States. presented at: *PM2000 Particulate Matter and Health – The Scientific Basis for Regulatory Decision-making Specialty Conference & Exhibition*. Air and Waste Management Association, Pittsburgh, 2000.

31. Thomas, A.; Gebhart, J. Correlations between gravimetry and light scattering photometry for atmospheric aerosols. *Atmos. Environ.* **1994**, *28*, 935-938.
32. Lilienfeld, P. Nephelometry, an ideal PM-2.5/10 method? In *Particulate Matter: Health and Regulatory Issues VIP-49*, Air and Waste Management Association, Pittsburgh, 1995; pp 211-225.
33. Husar, R.B.; Falke, S.R. The relationship between aerosol light scattering and fine mass. Report No. CX 824179-01. Center for Air Pollution Impact and Trend Analysis, St. Louis, Mo. Prepared for U.S. Environmental Protection Agency, Research Triangle Park, 1996.
34. Kerker, M. *The Scattering of Light and Other Electromagnetic Radiation*. Academic Press, 1969.
35. Bullrich, K. Scattered radiation in the atmosphere. *Adv. Geophys.* **1984**, *10*, 99-260.
36. Hanel, G. The real part of the mean complex refractive index and the mean density of samples of atmospheric aerosol particles. *Tellus* **1968**, *20*, 371-379.
37. Hanel, G.; Bullrich, K. Calculations of the spectral extinction coefficient of atmospheric aerosol particles with different complex refractive indices. *Beitr. Phys. Atmos.* **1970**, *43*, 202-207.
38. Shettle, E.P.; Fenn, R.W. Models of the aerosol of the lower atmosphere and the effects of humidity variations on their optical properties. Air Force Geophysics Laboratory Report, AFGL-TR-79-0214, September 1979.
39. Patterson, E.M. Optical properties of the crustal aerosol: relation to chemical and physical characteristics. *J. Geophys. Res.* **1981**, *86*, 3236-3246.
40. Gillespie, J.B.; Lindberg, J.D. Seasonal and geographic variations in imaginary refractive index of atmospheric particulate matter. *Appl. Opt.* **1992**, *12*, 2107-2111.
41. Diner, D.J.; Abdou, W.; Ackerman, T.; Conel, J.; Gordon, H.; Kahn, R.; Martonchik, J.; Paradise, S.; Wang, M.; West, R. MISR level 2 algorithm theoretical basis: Aerosol/surface product, part 1 (aerosol parameters), Rep. *AJPL-D11400, Rev. A*, Jet Propul. Lab., Pasadena, 1994.
42. Morawska, L.; Johnson, G.; Ristovski, Z.D.; Agranovski, V. Relation between particle mass and number for submicrometer airborne particles. *Atmos. Environ.* **1999**, *33*, 1983-1990.
43. John, W.; Wall, S.M.; Ondo, J.F.; Winklmayr, J.L. Modes in the aerosol size distribution of atmospheric inorganic aerosol. *Atmos. Environ.* **1990**, *24*, 2349-2359.
44. Dave, J. Subroutines for computing the parameters of the electromagnetic radiation scattered by a sphere. Report No. 320-3237, IBM Scientific Center, Palo Alto, 1968; pp 65.
45. Dave, J. Effect of coarseness of the integration increment on the calculation of the radiation scattered by polydisperse aerosols. *Appl. Opt.* **1969**, *8*, 1161-1167.
46. Jaggard, D.L.; Hill, C.; Shorthill, R.W.; Stuart, D.; Glantz, M.; Rosswog, F.; Taggart, B.; Hammond, S. Light scattering from particles of regular and irregular shape. *Atmos. Environ.* **1981**, *15*, 2511-2519.
47. Hill, S.C.; Hill, C.; Barber, P.W. Light scattering by size/shape distributions of soil particles and spheroids. *Appl. Opt.* **1984**, *23*, 1025-1031.
48. Mishchenko, M.I.; Travis, L.D.; Kahn, R.A.; West, R.A. Modeling phase functions for dustlike tropospheric aerosols using a shape mixture of randomly oriented polydisperse spheroids. *J. Geophys. Res.* **1997**, *102*, 16831-16847.
49. White, W.H.; Macias, E.S.; Nininger, R.C.; Schorran, D. Size-resolved measurements of light-scattering by ambient particles in the southwestern U.S.A. *Atmos. Environ.* **1994**, *28*, 900-921.

50. Tang, I.N. Chemical and size effects of hygroscopic aerosols on light scattering coefficients. *J. Geophys. Res.* **1996**, *101*, 19245-19250.
51. Malm, W.C.; Sisler, J.F.; Huffman, D.; Eldred, R.A.; Cahill, T.A. Spatial and seasonal trends in particle concentration and optical extinction in the United States. *J. Geophys. Res.* **1994**, *99*, 1347-1370.
52. Malm, W.C.; Molenaar, J.V.; Eldred, R.A.; Sisler, J.F. Examining the relationship among aerosols and light scattering and extinction in the Grand Canyon area. *J. Geophys. Res.* **1996**, *101*, 19251-19265.
53. Eldred, R.A.; Cahill, T.A.; Flocchini, R.G. Composition of PM_{2.5} and PM₁₀ aerosols in the IMPROVE network. *J. Air & Waste Manage. Assoc.* **1997**, *47*, 194-203.
54. Hering, S.; Cass, G. The magnitude of bias in the measurement of PM_{2.5} arising from volatilization of particulate nitrate from Teflon filters. *J. Air & Waste Manage. Assoc.* **1999**, *49*, 725-733.
55. Bergin, M.H.; Ogren, J.A.; Schwartz, S.E.; McInnes, L.M. Evaporation of ammonium nitrate aerosol in a heated nephelometer: implications for field measurements. *Environ. Sci. Technol.* **1997**, *21*, 2878-2883.
56. Dutcher, D.D.; Perry, K.D.; Cahill, T.A. Water and volatile particulate matter contributions to fine aerosol gravimetric mass. In *Visual Air Quality: Aerosols and Global Radiation Balance*, Air and Waste Management Association, Pittsburgh, 1997; pp 991-999.
57. Hanel, G. The properties of atmospheric aerosol particles as functions of the relative humidity at thermodynamic equilibrium with the surrounding moist air. *Adv. Geophys.* **1976**, *19*, 73-188.
58. Saxena, P.; Hildemann, L.M.; McMurry, P.H.; Seinfeld, J.H. Organics alter hygroscopic behavior of atmospheric particles. *J. Geophys. Res.* **1995**, *100*, 18755-18770.
59. Fuller, K.A.; Malm, W.C.; Kreidenweis, S.M. Effects of mixing on extinction by carbonaceous particles. *J. Geophys. Res.* **1999**, *104*, 15941-19954.
60. Malm, W.C.; Pitchford, M.L. Comparison of calculated sulfate scattering efficiencies as estimated from size-resolved particle measurements at three national locations. *Atmos. Environ.* **1997**, *31*, 1315-1325.
61. Richards, L.W.; Hurwitt, S.B.; McDade, C.; Couture, T.; Lowenthal, D.; Chow, J.C.; Watson, J. Optical properties of the San Joaquin valley aerosol collected during the 1995 integrated monitoring study. *Atmos. Environ.* **1999**, *33*, 4787-4795.
62. Heintzenberg, J.; Charlson, R.J. Design and Applications of the Integrating Nephelometer: A Review. *J. Atmos. Oceanic Technol.* **1996**, *13*, 987-1000.
63. Horvath, H.; Kaller, W. Calibration of integrating nephelometers in the post-halocarbon era. *Atmos. Environ.* **1994**, *28*, 1219-1223.
64. Anderson, T.L.; Covert, D.S.; Marshall, S.F.; Laucks, M.L.; Charlson, R.J.; Waggoner, A.P.; Ogren, J.A.; Caldow, R.; Holm, R.L.; Quant, F.R.; Sem, G.J.; Wiedensohler, A.; Ahlquist, N.A.; Bates, T.S. Performance characteristics of a high-sensitivity, three-wavelength, total scatter/backscatter nephelometer. *J. Atmos. Oceanic Technol.* **1996**, *13*, 967-986.
65. Molenaar, J.V. Analysis of the real world performance of the Optec NGN-2 ambient nephelometer. In *Visual Air Quality: Aerosols and Global Radiation Balance*, Air and Waste Management Association, Pittsburgh, Pa. 1997; pp 243-265.
66. Rosen, J.M.; Pinnick, R.G.; Garvey, D.M. Nephelometer optical response model for the interpretation of atmospheric aerosol measurements. *Appl. Opt.* **1997**, *36*, 2642-2649.

List of Key Words

PM_{2.5} mass

Aerosols

Optical properties

Measurements

“Integrating nephelometers”

“Light scattering photometers”